Supplementary Material

Exploring Ru/CeO_2 catalysts supported by ceria MOF-derived materials for improved ammonia synthesis and decomposition efficiency at mild conditions

Swati Singh[1,2], Seok-Jin Kim[3], Cafer Tayyar Yavuz[3], Mingwu Tan[4], Eswaravara Prasadarao Komarala[1], Kyriaki Polychronopoulou[1,2]

[1]Mechanical Engineering Department, Khalifa University, P.O. Box 127788, Abu Dhabi, United Arab Emirates.
[2]Center for Catalysis and Separations (CeCaS), Khalifa University, P.O. Box 127788, Abu Dhabi, United Arab Emirates.
[3]KAUST Catalysis Center, King Abdullah University of Science and Technology, Thuwal 23955-6900, Saudi Arabia.
[4]Institute of Sustainability for Chemicals, Energy and Environment (ISCE2), Agency for Science, Technology and Research (A*STAR), Jurong Island 627833, Singapore.

Correspondence to: Dr. Kyriaki Polychronopoulou, Mechanical Engineering Department, Khalifa University, P.O. Box 127788, Abu Dhabi, United Arab Emirates; Center for Catalysis and Separations (CeCaS), Khalifa University, P.O. Box 127788, Abu Dhabi, United Arab Emirates. E-mail: kyriaki.polychrono@ku.ac.ae

EXPERIMENTAL

Sample preparation

Synthesis of Ceria-MOF

In a typical procedure [28], $Ce(NO_3)_3 \cdot 6H_2O$ (1 mmol) and H3BTC (1 mmol) were mixed in an ethanol/water solution (50 mL, v/v = 1:1) under vigorous stirring at room temperature. The reaction mixture was then refluxed at 90 °C for 2 h. Finally, the white precipitate was collected by centrifugation, washed several times with ethanol and water, and dried at 60 °C. The XRD and

SEM of the prepared Ce-MOF is presented in **Figure S1-S2a-b**, confirming the successful preparation of Ce-MOF with nanorod morphology.

Ce-MOF was synthesized following a reported procedure [28] and subsequently calcined at 500 °C to obtain CeO_2. Ru-MOF was prepared via a solvothermal method using $RuCl_3$ and BTC. The nRu/CeO_2 catalysts were synthesized by sonication-assisted mixing of Ce-MOF and Ru-MOF precursors, followed by drying and calcination at 500 °C. Ru loading was varied between 0.2–2 wt.% and catalysts were denoted as nRu/CeO_2, where *n* represents the Ru content (wt.%). Detailed synthesis procedures are provided in the Supporting Information.

Synthesis of CeO_2 support

The prepared Ce-MOF was calcined at 500ºC to get CeO_2 support with a ramp of 10°C/min.

Synthesis of Ru-MOF

300 mg of $RuCl_3.3H_2O$ were dissolved to 92.5 ml of distilled water in a suitable container. 200 mg of BTC (benzene-1,3,5-tricarboxylic acid) were also added to the above solution, followed by the addition of0.5 ml of acetic acid. Allow the solution to stand for 30 minutes to ensure thorough mixing and dissolution of the components, resulting in a clear solution followed by a solution transfer to an autoclave. and the latter was maintained at 160°C for 72 hours to facilitate the synthesis process. After completion of the reaction, the autoclave was carefully removed, and it was allowed to cool down. The resulting product mixture was washed five times with water and ethanol to remove any impurities. After washing, dry the product under vacuum conditions for 24 hours at 150°C to remove any residual solvents and moisture.

Synthesis of Catalyst (nRu/CeO_2)

In the catalyst synthesis process, Ce-MOF and Ru-MOF precursors are individually sonicated for 30 minutes to ensure uniform dispersion. Subsequently, the two solutions are combined and further sonicated for an additional 2h to promote thorough mixing and interaction between the components. Following the mixture sonication step, the solution is centrifuged to separate any excess material or aggregates. Finally, the resulting mixture underwent vacuum drying at 60°C to remove any residual solvent and to obtain the desired composite material. This systematic procedure ensures the proper preparation and integration of Ce-MOF and Ru-MOF components, leading to the

formation of a well-defined and functional composite material. The as prepared material was calcined at 500ºC to obtain the final catalyst (nRu/CeO_2). In the experimental procedure, the loading of Ru-MOF was systematically varied across a range of 0.2 to 2 wt.% relative to the total weight of the final catalyst. The resulting catalysts were designated with the notation "nRu/CeO_2," where "n" represents the weight percentage of Ru-MOF loading. For example, a catalyst prepared with 0.2wt.% Ru-MOF loading would be labelled as "0.2Ru/CeO_2."

Characterization details

ex-situ characterization analysis

ICP. For the most demanding trace elemental analyses, the Thermo Scientific™ iCAP™ 7600 ICP-OES (Inductively Coupled Plasma-Optical Emission Spectroscopy), was used. The airflow rate of 25 L/min, argon flow rate of 13.0 L/min and nitrogen flow rate of 1.4 L/min were used for the analysis. 100 mg of the as-prepared catalyst was used for the analysis. Before analysis, the samples were first digested in concentrated aqua regia (3:1 HCl:HNO_3) to ensure complete dissolution of CeO_2 and Ru-containing species. The resulting digest was then diluted by mixing 10 mL of the solution with 40 mL of deionised water, yielding a total of 50 mL containing approximately 20% concentrated acid. This diluted solution was used for ICP-OES analysis, as concentrated acids are incompatible with the instrument's operating conditions.

X-ray diffraction (**XRD**) analysis was conducted on a small sample of the catalysts using a Cu Kα radiation source with a wavelength of 1.5406 Å. The XRD examination was performed in a reflection mode at 45 kV and 40 mA on an X'Pert PRO powder diffractometer, with a step time of 10 s and a step size of 0.02°. A zero-background holder was employed to reduce scanning noise, and the analysis covered the 2θ range of 5-80°.

Raman spectra were attained using Witec Alpha 300 RA, Ulm, Germany, with a 532 nm laser. Surface area and pore volume measurements of the prepared catalysts were carried out under cryogenic conditions (77 K) using 3Flex Micromeritics adsorption unit. Before the Brunauer–Emmett–Teller (**BET**) analysis, the catalyst samples underwent an 8-hour degassing under vacuum at 120 °C to remove adsorbed water and/or other impurities without causing irreversible changes to the catalyst surface. The BET method was applied to calculate the surface area for relative

pressure ranging from 0.05 to 0.3. The Barrett–Joyner–Halenda (BJH) method was employed to derive pore volume and pore size distribution.

TEM: The reduced catalysts were prepared following in-situ reduction at 800°C, using a N_2/H_2 (1/3) gas mixture. After reduction, a small amount of powder from each catalyst was mixed with 99.8% ethanol (POCH) to form a slurry. The latter was then placed in an ultrasonic homogenizer for 20 seconds. After homogenization, the catalyst-containing slurry was pipetted onto a 200-mesh copper grid, which was covered with lacey formvar and stabilized with carbon (Ted Pella Company). The grid was left on filter paper to allow the ethanol to evaporate. Once the samples had dried, they were transferred onto a single-tilt holder and placed in the electron microscope for analysis. High-angle annular dark field scanning TEM (HAADF-STEM), high-resolution transmission electron microscopy (HRTEM), and element mapping images were acquired by using an FEI TITAN Cs-corrected ChemiSTEM. Post catalytic samples were analyzed using High-resolution transmission electron microscopy (HR-TEM) using a Titan 80-300 ST microscope from Thermo-Fisher Scientific. The microscope was operated at an accelerating voltage of 300 kV.

The H_2 temperature-programmed desorption (**H_2-TPD)** technique was used to study the dispersion of the supported Ru catalysts. 70 mg of sample was loaded in the U-tube microreactor, and the temperature was increased under He gas flow up to 800ºC. At these conditions, reduction of the sample took place in hydrogen gas flow (1 bar) at 800ºC /1h, followed by He purge at 800ºC until the H_2-TCD signal was stabilized at its background value. The catalyst was cooled down to 30ºC in He flows; then, 30-min of exposure to a 0.5 vol.% H_2/He adsorption gas followed. After H_2 chemisorption, the sample was purged in He flows for 10 min, and its temperature was then increased to 800ºC ($\beta = 30$ºC min^{-1}, H_2-TPD). The H_2 signal ($m/z = 2$) was continuously monitored with a thermal conductivity detector (TCD) and converted into concentration (mol%) using a certified gas mixture (0.95 vol% H_2/He).

H_2 temperature-programmed reduction (**H_2-TPR**) was used to monitor the catalyst's reducibility. Approximately 70 mg of the catalyst sample was placed in a U-shaped tubular reactor in the AutoChem 2920 chemisorption unit. The catalyst underwent oxidation with a mixture of 20 vol % O_2 and He at 300 °C, followed by evacuation and cooling in pure He gas before treatment with 10 vol% H_2/Ar gas. The temperature was raised from ambient to 800 °C at a rate of 10 °C/min, and the H_2 signal was continuously monitored using a thermal conductivity detector (TCD).

X-ray photoelectron spectroscopy (**XPS**) studies were performed on reduced samples (under H_2/Ar at 700ºC) using an ESCALAB Thermo Scientific Theta Probe Angle-Resolved X-ray Photoelectron Spectrometer in East Grinstead, UK. An Al Kα X-ray source with a photon energy of 1486.6 eV was utilized. Survey spectra were collected with a pass energy of 100 eV, while high-resolution core-level spectra were acquired with a pass energy of 50 eV. The C 1s peak at 284.8 eV was used as an internal reference for calibration. XPS analysis provided insights into the surface chemical composition and oxidation states of elements in the ex situ-reduced catalysts.

in-situ characterization analysis

The **XRD** analysis was performed using an INEL EQUINOX 3000 X-Ray Diffractometer equipped with an XRK900 Reactor Chamber for in-situ measurements. The analysis was conducted on Ru/CeO_2 catalysts with varying nominal wt.% Ru loadings of 0.2Ru, 0.5Ru, and 1Ru. To study the structural evolution of the catalysts under reduction conditions, the samples were exposed to a H_2/N_2 (3:1) gas mixture. Initially, XRD patterns were recorded at room temperature to obtain baseline data. The temperature was then gradually ramped at 20ºC/min increased in steps, with each step followed by an XRD analysis. The temperature was raised first to 200°C, where it was held for 1 hour, followed by XRD analysis under the reduction atmosphere. The same procedure was repeated at 400°C, 600°C, and 700°C, with each step maintaining the temperature for 1 hour before conducting another XRD scan. Final scan was done after the sample was cooled down to room temperature (RT). This stepwise heating allowed for the observation of changes in the crystallinity, phase transitions, and structural evolution of the Ru/CeO_2 catalysts under reduction conditions.

High-resolution **XPS** measurements were conducted on a ULVAC-PHI Genesis 900 system, equipped with a Prevac Flow-through High Pressure Reactor and ultrahigh vacuum (UHV) chambers. The analysis focused on the elements of interest, namely Ru, Ce, and O, in the Ru/CeO_2 catalysts with varying nominal wt.% Ru loadings (0.2Ru, 0.5Ru, 1Ru). For each sample, XPS analysis was initially performed at RT, followed by measurements under reduction gas conditions. The temperature was then increased to 700°C for 2 hours, with XPS analysis conducted under the atmosphere (H_2/N_2 = 3:1). Subsequently, the temperature was reduced back to 400°C, and further XPS analysis was carried out under the reaction gas conditions (H_2/N_2 = 3:1). All binding energies were calibrated using the surface adventitious carbon 1s peak at 284.4 eV as the reference.

Evaluation of catalytic performance

NH_3 Synthesis Assessment

The preparation for the catalytic activity test involves diluting 67.5 mg of the catalyst with 500 mL of coarse silicon carbide (46 grit, Alfa Aesar, Lot: 10226827). A quartz tube reactor (inner diameter (ID) of 2 mm and an outer diameter (OD) of 3 mm) equipped with a porosity 3 (por. 3) filter was used and then inserted into Flowrence XD (Avantium). The test was performed at a weight hourly space velocity (WHSV) of 10,000 mL/g/h, with a feed gas mixture of 25% N2 (99.999% purity) and 75% H2 (99.999% purity). Helium (He, 99.999%) was added as an internal standard to calculate the ammonia flow in the outlet. The concentration of the outlet NH3 is analyzed using a thermal conductivity detector (TCD) by an online gas chromatogram (8890 GC system, Agilent). The initial screening test was conducted under various conditions, including a gas flow of 10,000 mL/g/h, pressure ranging from 10 to 50 bar at 400 °C. Prior to the test, the catalyst was reduced under a mixture of 75% H2 and 25% N2 at 800 °C for 12 hours. During the reaction, the gas flow rates were set to 2.5 mL/min for N2, 7.5 mL/min for H2, and 1.25 mL/min for He. The reaction temperature was maintained at 400 °C, and the pressure was varied between 10 bar and 50 bar to observe the catalytic performance under different pressure conditions.

NH_3 catalytic cracking assessment

For the ammonia catalytic decomposition test, 23 mg of the catalyst was diluted with 500 μL of coarse silicon carbide. The reduction process was carried out in a gas mixture containing 75% H_2 and 25% N_2 at 700 °C for 12 hours. The NH_3 cracking reaction was carried out in a quartz tube reactor (ID: 2 mm, OD: 3 mm, with por. 3 filter) at a WHSV of 24,000 mL/g/h, over a temperature range from 350–550 °C. NH_3 was introduced at a flow rate of 13.5 mL/min, with 1.25 mL/min of He as internal standard gas.

Stability of NH_3 synthesis activity test

A long-term stability test was conducted using 20 mg of catalyst loaded in the same quartz tube reactor (ID: 2 mm, OD: 3 mm, with por. 3 filter). Before the test, the catalyst was reduced under a 75% H_2 and 25% N_2 at 800 °C for 5 hours. The stability test was performed under continuous operation for 150 hours at a constant temperature of 400 °C and a pressure of 50 bar. The gas feed composition was maintained at 3.75 mL/min of N_2, 11.25 mL/min of H_2, and 1.25 mL/min of He. Outlet ammonia concentrations were monitored to evaluate catalyst durability.

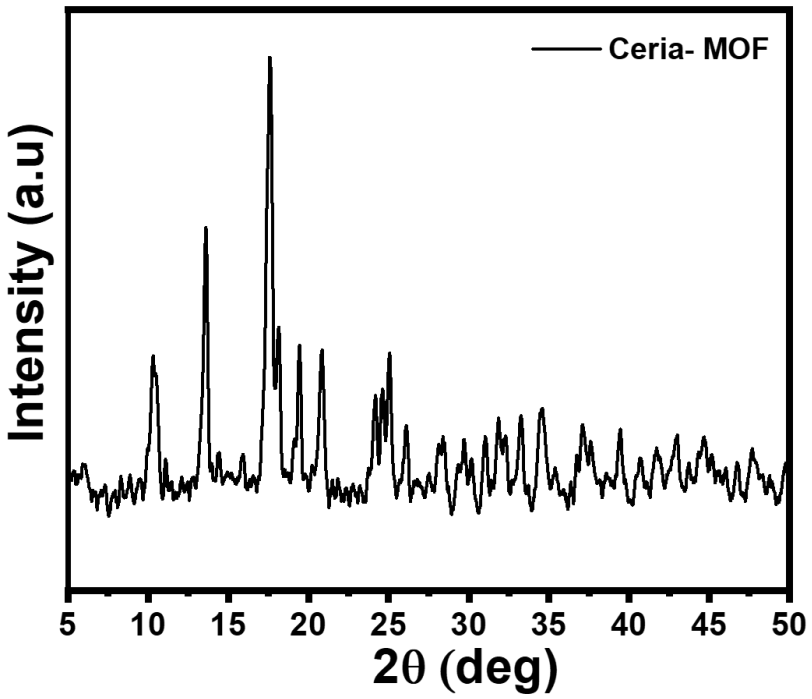

Figure S1. XRD patterns of Ce-MOF

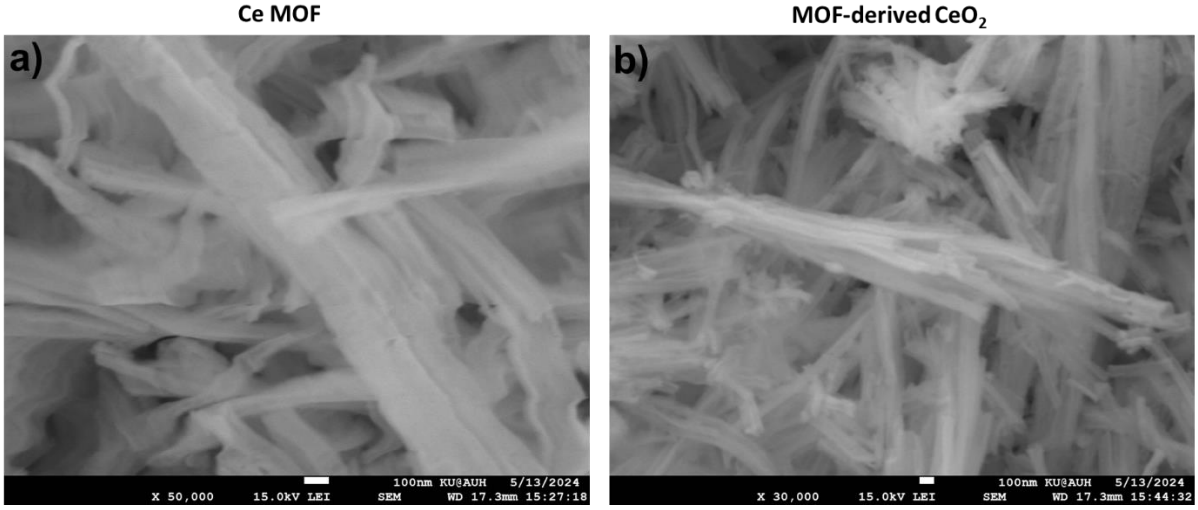

Figure S2. SEM micrographs of **a)** Ce MOF, and **b)** MOF-derived CeO_2.

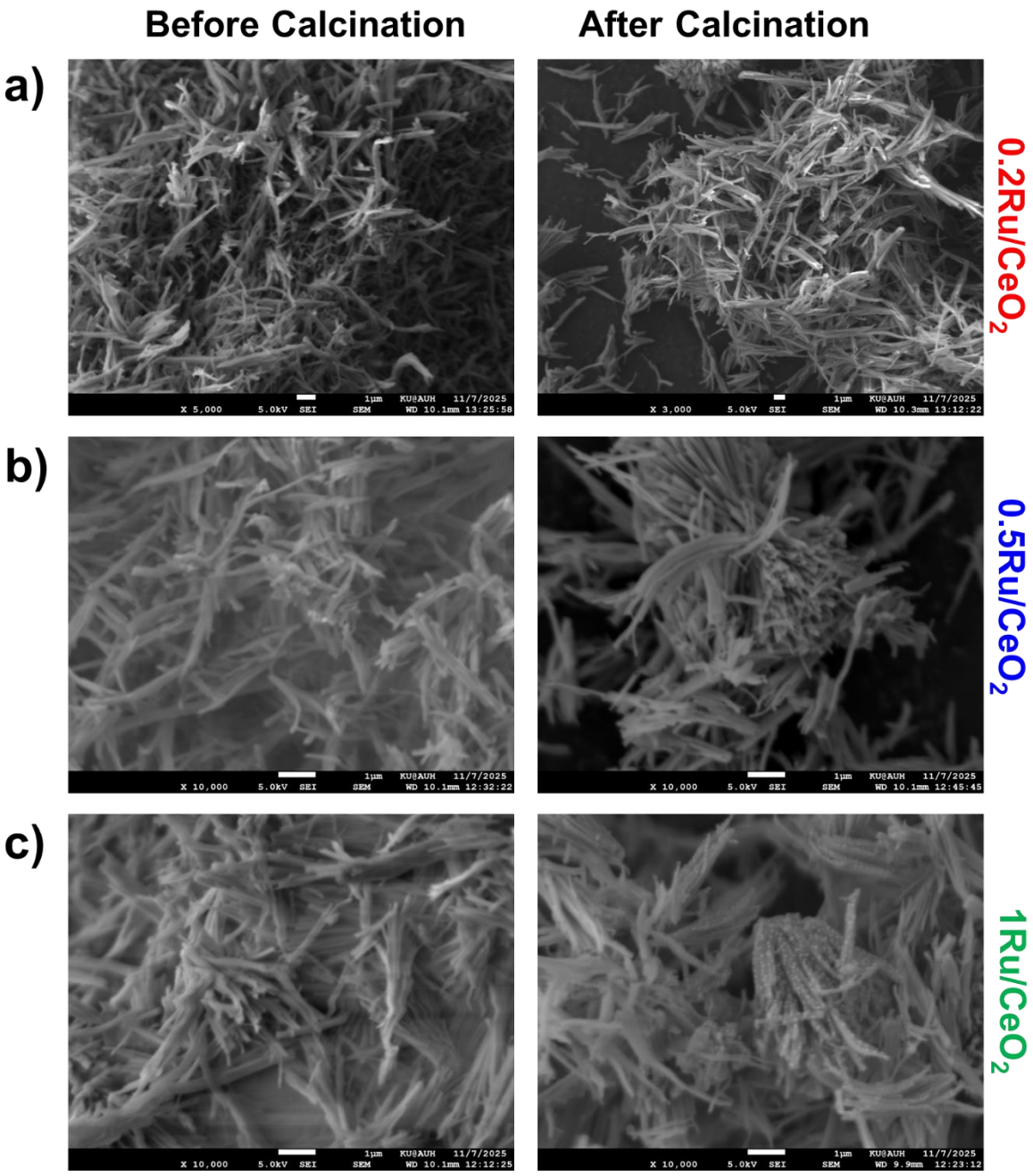

Figure S3. SEM micrographs of catalysts before/after calcination: a) 0.2Ru, b) 0.5Ru, and c) 1Ru catalyst.

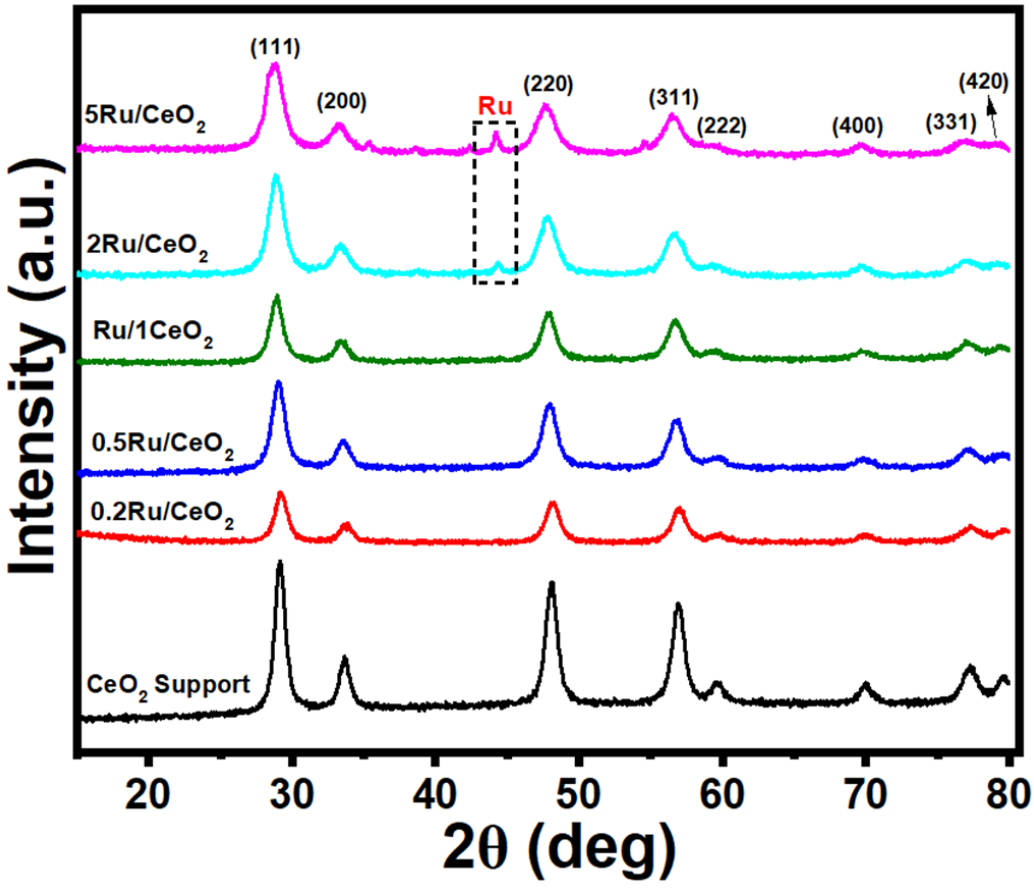

Figure S4. XRD profile of as prepared CeO_2 support and nRu/CeO_2 catalysts (n=0.2, 0.5, 1, and 2).

Figure S4 displays the XRD patterns of the as-prepared CeO_2 supports and their corresponding nRu/CeO_2 catalysts. The XRD patterns of the CeO_2 supports are consistent with the cubic fluorite structure of CeO_2 (JCPDS 34-0394) [1], with characteristic 2θ angles at 29.14°, 33.7°, 48.0°, 56.8°, 59.6°, 70.0°, 77.2°, and 79.6°, corresponding to the (111), (200), (220), (311), (222), (400), (331), and (420) planes, respectively. No peaks indicative of impurities was observed, confirming the high purity of the synthesized CeO_2. In the XRD patterns of the nRu/CeO_2 catalysts, no diffraction peaks associated with Ru species (such as metallic Ru at 44° or RuO_x at 35° and 54°) were detected, likely due to the small particle size of Ru, as confirmed by HRTEM analysis **(Figure 6)** [2] [3]**.** This small particle size prevents detection via XRD [4]. However, the 2Ru/CeO_2 catalyst exhibits a peak around 2θ = 44°, corresponding to the (101) planes of metallic Ru (JCPDS 06-0663) [5], which is attributed to phase separation during the calcination process [6].

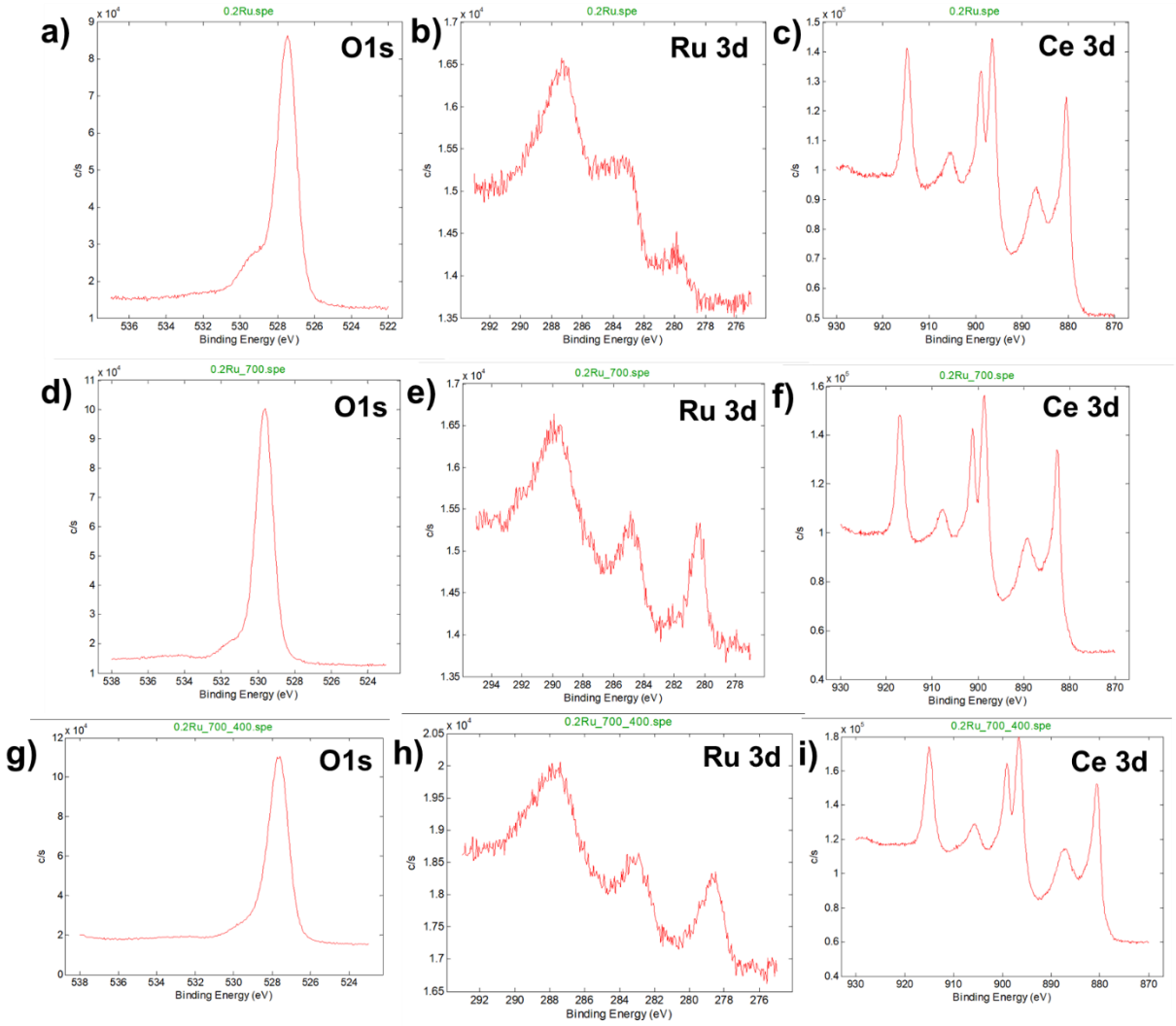

Figure S5. XPS spectra of 0.2Ru/CeO_2 for O1s, Ru 3d, and Ce 3d at **(a-c)** 25ºC, **(d-f)** 700ºC, and **(g-i)** 400ºC.

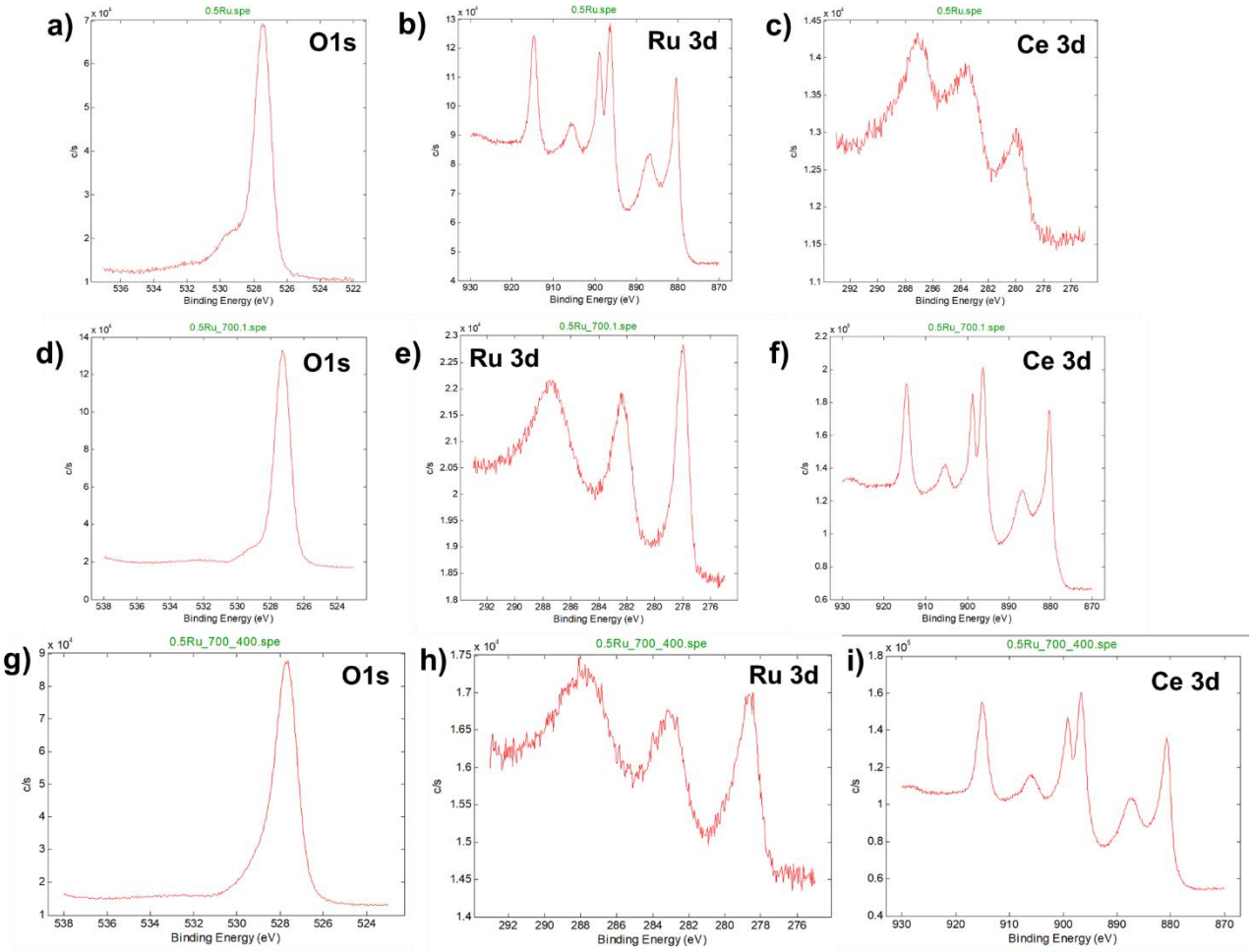

Figure S6. XPS spectra of 0.5Ru/CeO_2 for O1s, Ru 3d, and Ce 3d at **(a-c)** 25ºC, **(d-f)** 700ºC, and **(g-i)** 400ºC.

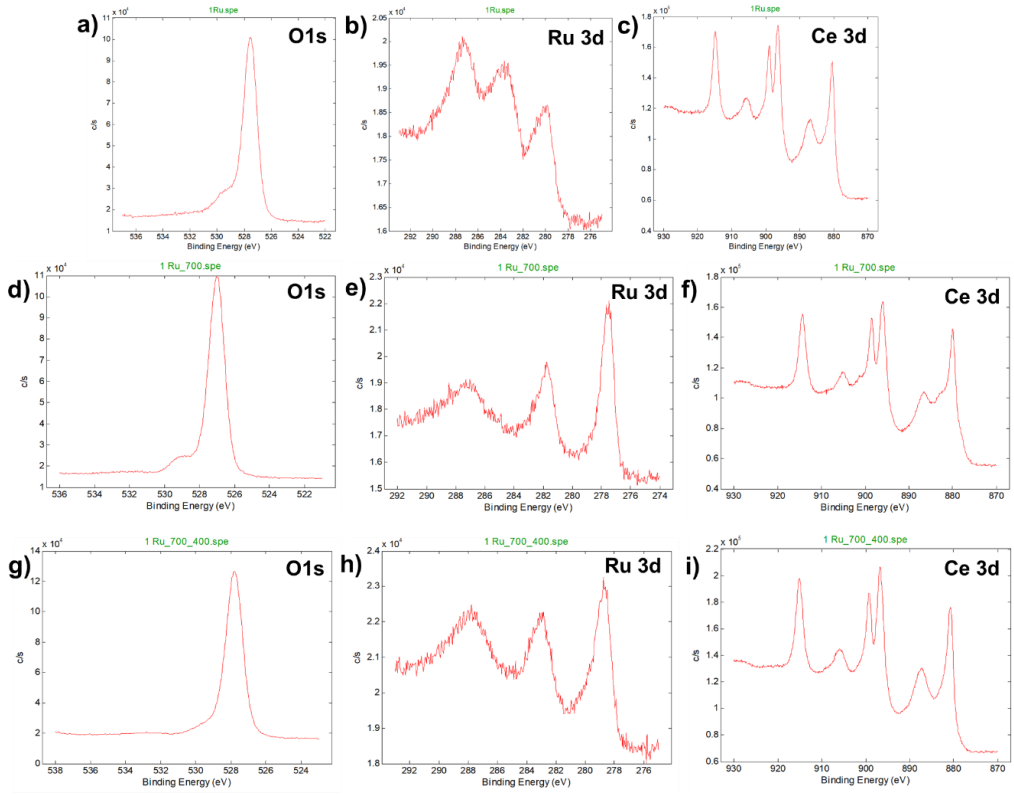

Figure S7. XPS spectra of 1Ru/CeO_2 for O1s, Ru 3d, and Ce 3d at **(a-c)** 25ºC, **(d-f)** 700ºC, and **(g-i)** 400ºC.

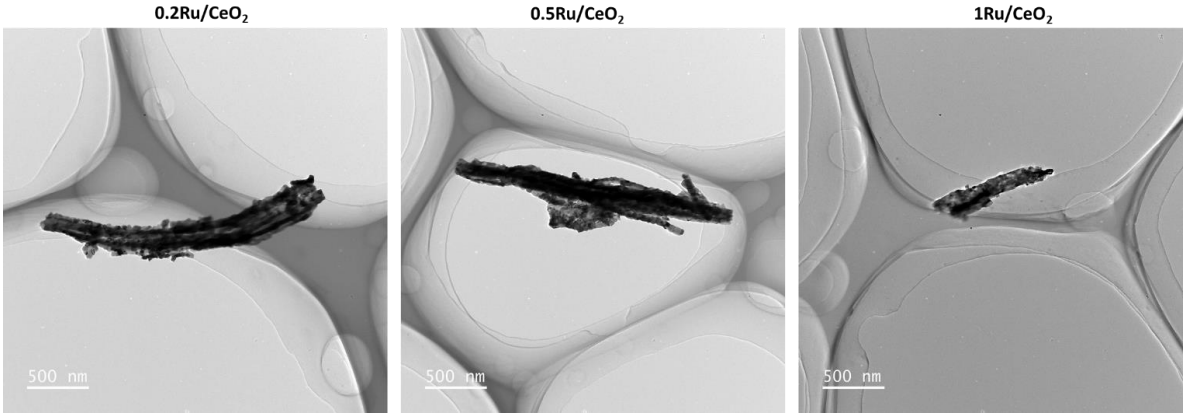

Figure S8. HRTEM images of nRu/CeO_2 catalysts (n=0.2, 0.5, and 1 wt%).

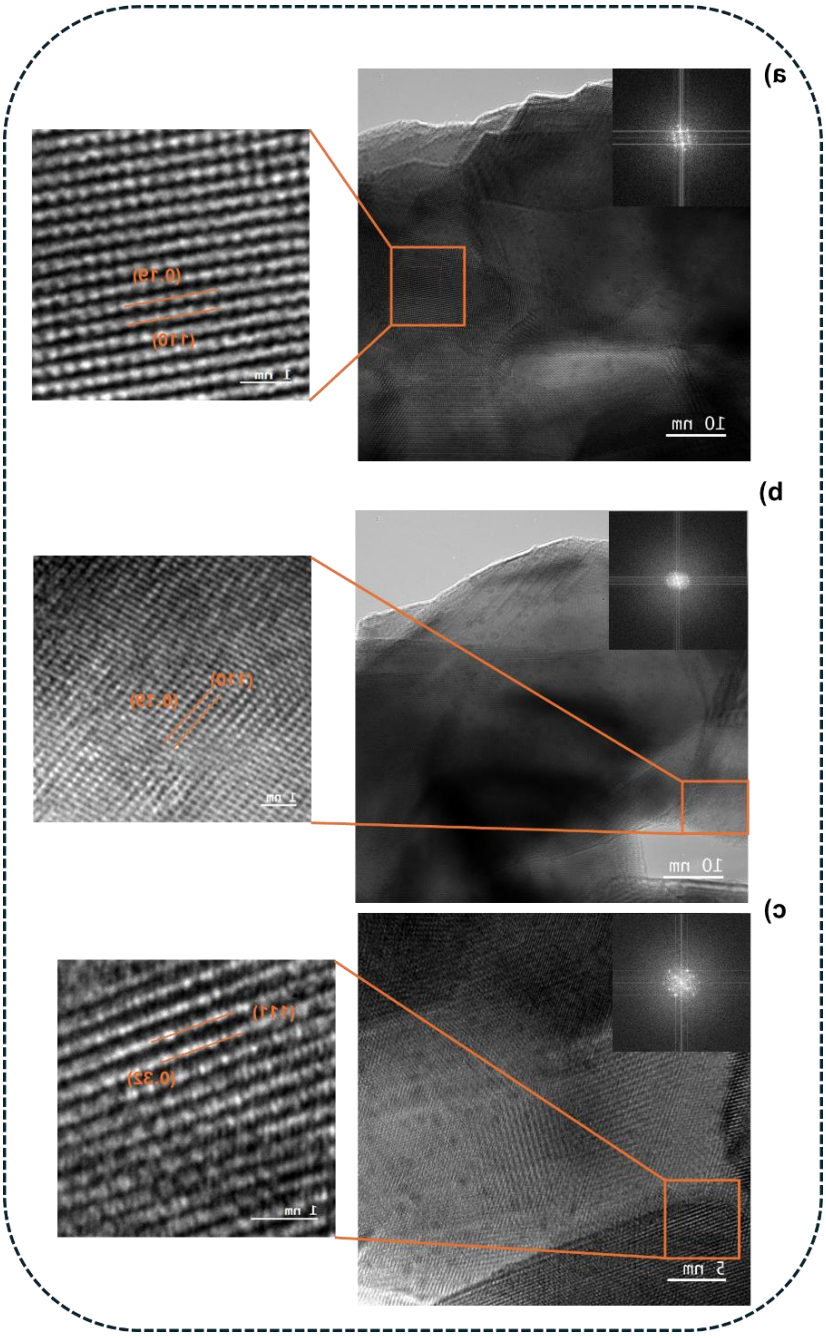

Figure S9. High-resolution TEM images of the reduced 0.5Ru/CeO_2 catalyst. (a–c) Representative regions showing well-resolved lattice fringes indexed to CeO_2 (110) and (111) planes with d-spacings of ~0.19 and ~0.31 nm, respectively, together with the corresponding FFT patterns (insets), confirming the high crystallinity and preserved fluorite structure of the CeO_2 support after reduction.

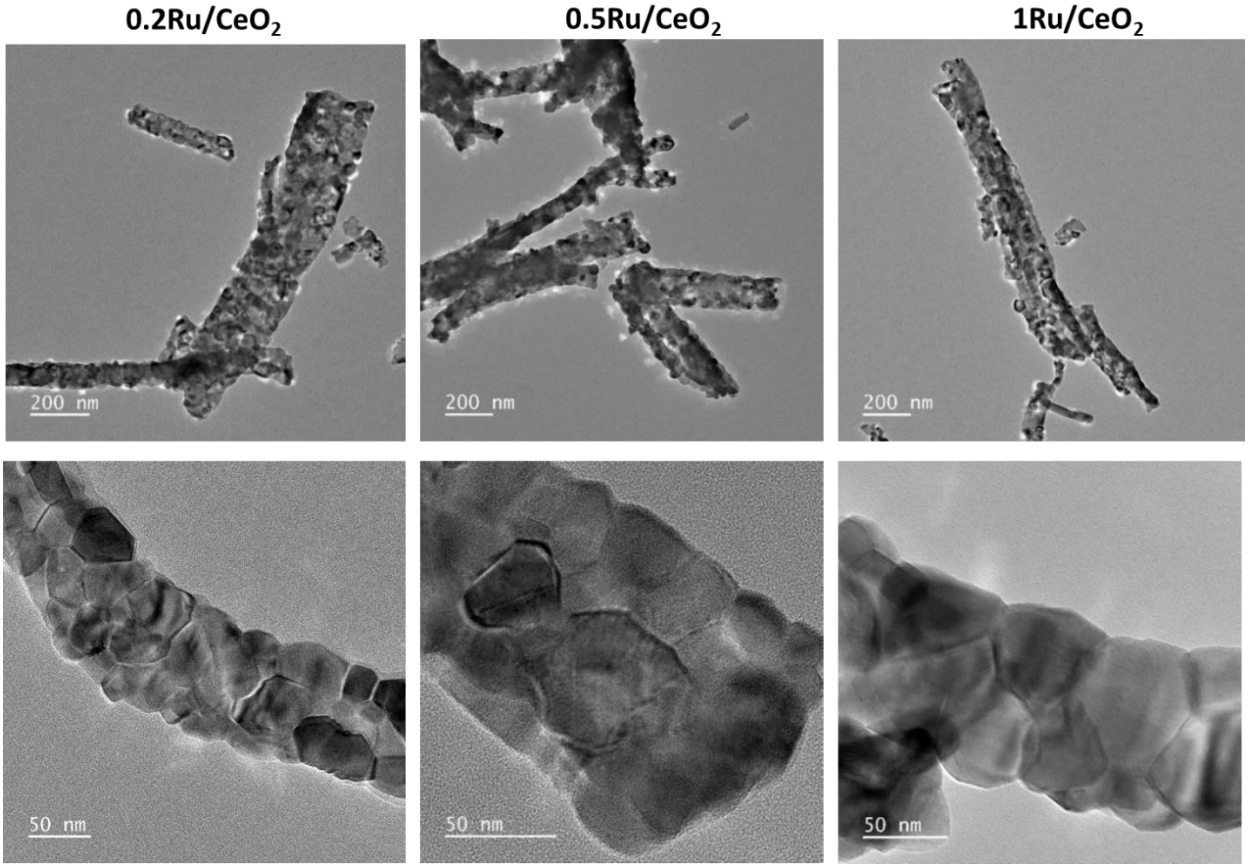

Figure S10. HRTEM of a) 0.2Ru/CeO_2, b) 0.5Ru/CeO_2, and 1Ru/CeO_2 catalysts after catalytic activity test.

Table S1. Ru particle size as obtained from the H_2 chemisorption studies. [a]Nanoparticle size of Ru metal derived from HRTEM.

Catalyst	Metal surface area (m^2/g)	Crystallite size (nm)
$0.2Ru/CeO_2$	34.5	14 (0.9[a])
$0.5Ru/CeO_2$	11.1	43 (1.06[a])
$1Ru/CeO_2$	10.9	44(1.2[a])

The crystallite sizes (Table S1) obtained from the H_2-TPD analysis are 14 nm, 43 nm, and 44 nm for $0.2Ru/CeO_2$, $0.5Ru/CeO_2$, and $1Ru/CeO_2$, respectively. These values are significantly higher than those calculated from the HRTEM studies, which will be discussed later. This discrepancy arises because H_2-TPD tends to overestimate the crystallite size, primarily due to Ru promoting H_2 spillover onto the CeO_2 support; the latter leading to a stored amount of hydrogen into ceria. Therefore, CO-TPD is considered a more suitable alternative technique for accurately assessing the crystallite size of such type of catalysts.

Table S2. NH_3 production rate of nRu/CeO_2 (n=0.2, 0.5, 1, and 2) at 400ºC and P= 10-50 bar.

Catalyst	**1615 ± 118.8 NH_3 production rate (µmol g^{-1} h^{-1}) 2690 ± 28.1 3150 ± 35.8**				
	10 bar	**20 bar**	**30 bar**	**40 bar**	**50 bar**
CeO_2 Support	x	x	311 ± 11.0	354 ± 7.9	374 ± 11.3
$0.2Ru/CeO_2$	1615 ± 118.8	2031 ± 46.7	2316 ± 29.3	2690 ± 28.1	3150 ± 35.8
$0.5Ru/CeO_2$	2811 ± 47.5	3448 ± 35.6	3908 ± 23.4	4631 ± 44.2	4665 ± 58.9
$1Ru/CeO_2$	2080 ± 48.1	2609 ± 20.9	2992 ± 32.2	3826 ± 18.5	3831 ± 34.3
$2Ru/CeO_2$	621 ± 90.6	974 ± 41.6	1400 ± 26.3	1963 ± 51.6	2807 ± 12.6

Table S3. NH_3 production rate of various reported Ru/CeO_2-based catalysts

S.No.	Catalyst	Ru (wt.%)	T (°C)	P (Bar)	NH_3 yield (μmol $g_{cat}^{-1}h^{-1}$)	NH_3 yield/Ru (wt.%)	Ref
1	$0.2Ru/CeO_2$	0.22	400	10	1615	7340	*This Work*
2	$0.2Ru/CeO_2$	0.22	400	50	3150	14318	*This Work*
3	$0.5Ru/CeO_2$	0.35	400	10	2811	8031	*This Work*
4	$0.5Ru/CeO_2$	0.35	400	50	4655	13300	*This Work*
5	Ru/CeO_2-TPAOH	2.5	450	30	22000	8800	[7]
6	Ru/CeO_2-EDA	2.5	450	30	19000	7600	[7]
7	Ru/CeO_2–NaOH	2.5	450	30	16500	6600	[7]
8	$Ru/r\text{-}CeO_2$	4	400	10	3830	957.5	[8]
9	$Ru/c\text{-}CeO_2$	4	400	10	1289	322.2	[8]
10	$Ru/p\text{-}CeO_2$	4	400	10	529	132.5	[8]
11	$2.8Ru\text{-}CeO_2$	2.8	400	10	10400	3714.2	[9]
12	Ru/CeO_2-H	1	400	10	3987	3987	[10]
13	Ru/CeO_2-BH	1	400	10	5454	5454	[10]
14	$Na\text{-}Ru/CeO_2$-H	1	400	10	2352	2352	[10]
15	Ru/CeO_2–CS	2.5	450	30	27000	10800	[11]
16	Ru/CeO_2–MS	2.5	450	30	21000	8400	[11]
17	Ru/CeO_2–NR	2.5	450	30	15000	6000	[11]
18	Ru/CeO_2-r	10	400	10	18000	1800	[12]
19	Ru/CeO_2-c	10	400	10	7900	790	[12]
20	Ru/CeO_2	5	390	9	7200	1440	[13]
21	$2K\text{-}Ru/r\text{-}CeO_2$	4	400	10	11200	2800	[8]
22	$2Ba\text{-}Ru/r\text{-}CeO_2$	4	400	10	6600	1650	[8]
23	$Ru@CeO_2$-9	2.48	425	10	13 504	5445	[14]
24	Ru/CeO_2-CP	2.48	425	10	7860	3169	[14]
25	Ru clusters/CeO_2	5	400	10	20720	4144	[15]
26	Ba-Cs-Ru/C[m]	9.1	400	90	68 500	7527	[16]
27	Mittasch's Fe[n]	40.5	460	150	95 600	2360	[17]

Table S4. Lattice parameters of nRu/CeO_2 catalysts (n=0.2, 0.5, 1, and 2). [a]using Bragg's Law, calculated by (111) facet from XRD patterns for catalysts before and after reaction, [b]using Scherrer Equation.

Catalyst before reaction	**2Θ (111)**	**d-spacing (Å)[a]**	**Lattice constant *a* (nm)**	**Crystallite Size (nm)[b]**
0.2Ru/CeO_2	28.8	3.08	0.53	28.0
0.5Ru/CeO_2	28.9	3.09		21.8
1Ru/CeO_2	28.9	3.09		21.0
Catalyst after reaction	**2Θ (111)**	**d-spacing (Å)[a]**		**Crystallite Size (nm)[b]**
0.2Ru/CeO_2	28.5	3.12	0.54	25.55
0.5Ru/CeO_2	28.5	3.12		29.87
1Ru/CeO_2	28.5	3.12		29.68

References

1. Guan, Y., et al., *Promotion of CO2 Electroreduction on Bismuth Nanosheets with Cerium Oxide nanoparticles.* Chemistry – An Asian Journal, 2024. **19**(17): p. e202400296.
2. Wang, F., et al., *Catalytic behavior of supported Ru nanoparticles on the {100}, {110}, and {111} facet of CeO2.* Journal of Catalysis, 2015. **329**: p. 177-186.
3. Sakpal, T. and L. Lefferts, *Structure-dependent activity of CeO2 supported Ru catalysts for CO2 methanation.* Journal of Catalysis, 2018. **367**: p. 171-180.
4. Huang, H., Q. Dai, and X. Wang, *Morphology effect of Ru/CeO2 catalysts for the catalytic combustion of chlorobenzene.* Applied Catalysis B: Environmental, 2014. **158-159**: p. 96-105.
5. Okal, J. and K. Adamska, *Thermal Stability of Ru–Re NPs in H2 and O2 Atmosphere and Their Activity in VOCs Oxidation: Effect of Ru Precursor.* Catalysis Letters, 2022. **152**(1): p. 55-74.
6. Sivan, S.E., et al., *Facile MOF-derived one-pot synthetic approach toward Ru single atoms, nanoclusters, and nanoparticles dispersed on CeO2 supports for enhanced ammonia synthesis.* Journal of Catalysis, 2022. **408**: p. 316-328.
7. Li, W., et al., *Influence of CeO2 supports prepared with different precipitants over Ru/CeO2 catalysts for ammonia synthesis.* Solid State Sciences, 2020. **99**: p. 105983.
8. Ma, Z., et al., *New insights into the support morphology-dependent ammonia synthesis activity of Ru/CeO 2 catalysts.* Catalysis Science & Technology, 2017. **7**(1): p. 191-199.

9. Sivan, S.E., et al., *Facile MOF-derived one-pot synthetic approach toward Ru single atoms, nanoclusters, and nanoparticles dispersed on CeO2 supports for enhanced ammonia synthesis.* Journal of Catalysis, 2022. **408**: p. 316-328.
10. Li, C., et al., *Improving the ammonia synthesis activity of Ru/CeO2 through enhancement of the metal–support interaction.* Journal of Energy Chemistry, 2021. **60**: p. 403-409.
11. Liu, P., et al., *Morphology effect of ceria on the ammonia synthesis activity of Ru/CeO 2 catalysts.* Catalysis Letters, 2019. **149**: p. 1007-1016.
12. Lin, B., et al., *Morphology effect of ceria on the catalytic performances of Ru/CeO2 catalysts for ammonia synthesis.* Industrial & Engineering Chemistry Research, 2018. **57**(28): p. 9127-9135.
13. Sato, K., et al., *A low-crystalline ruthenium nano-layer supported on praseodymium oxide as an active catalyst for ammonia synthesis.* Chemical science, 2017. **8**(1): p. 674-679.
14. Wang, X., et al., *Efficient ammonia synthesis over a core–shell Ru/CeO 2 catalyst with a tunable CeO 2 size: DFT calculations and XAS spectroscopy studies.* Inorganic Chemistry Frontiers, 2019. **6**(2): p. 396-406.
15. Feng, J., et al., *Sub-nanometer Ru clusters on ceria nanorods as efficient catalysts for ammonia synthesis under mild conditions.* ACS Sustainable Chemistry & Engineering, 2022. **10**(31): p. 10181-10191.
16. Kowalczyk, Z., et al., *Carbon-based ruthenium catalyst for ammonia synthesis: Role of the barium and caesium promoters and carbon support.* Applied Catalysis A: General, 2003. **248**(1-2): p. 67-73.
17. Zheng, J., et al., *Efficient non-dissociative activation of dinitrogen to ammonia over lithium-promoted ruthenium nanoparticles at low pressure.* Angewandte Chemie International Edition, 2019. **58**(48): p. 17335-17341.